Acoustic-optic techniques for phased-array antenna processing

Riza, Nabeel

Nabeel Agha Riza, "Acoustic-optic techniques for phased-array antenna processing," Proc. SPIE 1622, Emerging Optoelectronic Technologies, (16 December 1992); doi: 10.1117/12.636810

SPIE.

Event: Emerging OE Technologies, Bangalore, India, 1991, Bangalore, India

Acousto-Optic Techniques for Phased Array Antenna Processing

Nabeel A. Riza
General Electric Corporate Research and Development
P.O. Box 8, Schenectady, New York 12301, U.S.A.

Abstract

An acousto-optic phased array antenna beamformer with independent phase and carrier control capability is experimentally demonstrated using single-sideband signals driving two acousto-optic devices. A dynamic range of 66.6 dB @+2 MHz and carrier-to-noise of 126.9 dB/Hz @+2 MHz is measured. This beamformer has wide antenna tunable bandwidth and intrapulse beamforming capabilities.

I. Introduction

Phase-based optical beamformers employ the phenomenon of controlled optical interference, with the particular interference/phase pattern oscillating in time at the desired radar microwave frequency [1,2]. By spatially sampling this interference pattern with a fiber/detector array, it is possible to simultaneously generate all the correctly phased signals for pointing the array antenna beam in a desired direction. It is widely known that optical interferometers are highly sensitive to mechanical vibrations and other system instabilities, which in turn leads to phase instabilities in the output microwave signal.

Recently, we proposed and experimentally demonstrated a novel in-line additive acousto-optic (AO) beamforming architecture that has excellent interferometric/phase stability [2-4]. One unique property of this AO beamformer that was experimentally demonstrated was the position coding of the phased array signals by frequency coding the carrier frequency. In other words, depending on the desired antenna beam position, the carrier was offset by a certain frequency interval. Sometimes it is desirable to have mutually independent phase and carrier control; for instance, when operating within a limited radar band, or when intrapulse beamforming is required to prevent beam squint when transmitting long-duration frequency modulated signals. In this paper, we demonstrate a technique using single-sideband (SSB) signals to generate independent carrier and phase control from the AO beamformer [2].

II. Single-Sideband Processing Concept and Laboratory Setup

The basic AO system is shown in Fig. 1. To illustrate the principle of SSB processing, the experiment is performed at a 120-MHz rf carrier using 60-MHz center frequency, 10-μs aperture, flint glass acousto-optic devices (AODs). To obtain the desired independent carrier and phase control from the AO processor, an upper sideband (USB) signal of frequency $\omega_c+\omega_o$ is fed to AOD1, and a lower sideband (LSB) signal of frequency $\omega_c-\omega_o$ is fed to AOD2. Here ω_c is the 60-MHz AOD center frequency and ω_o is the phase control parameter in kilohertz.

A 10-mW He-Ne laser beam, after expansion and collimation, passes through an iris that controls the illuminated aperture of AOD1. The illuminated acoustic column is 16 mm in length and 4.5 mm in height. AOD1's acoustic column is Bragg matched to the incident beam such that a positive doppler shifted +1 diffracted order beam with an optical frequency of $\nu+\omega_c+\omega_o$ is generated from AOD1. Here ν is the optical frequency of the laser. Note that compared with the undiffracted (DC) beam, the +1 order not only suffers a shift in the optical frequency, but also undergoes a spatial shift or beam deflection that is proportional to the rf frequency $\omega_c+\omega_o$. Both the DC and +1 order beams are 1:1 imaged onto AOD2 using two 15-cm focal length (FL) spherical lenses. The acoustic column of AOD2 is Bragg matched to the DC beam from AOD1 such that a negative doppler –1 order diffracted beam with an optical frequency of $\nu-[\omega_c-\omega_o]$ is produced from AOD2. Again, the –1 order has a spatial deflection that is proportional to the rf frequency $\omega_c-\omega_o$. Note that the +1 order from AOD1 passes essentially unaffected through AOD2, and is almost collinear with the –1 order. The –1 and +1 orders are imaged onto the fiber/detector plane using a 10-cm FL spherical lens that provides a 2X magnification along the x, or acoustic vector, direction, and a 15-cm FL cylindrical lens that collimates the diffracted orders along the AOD height

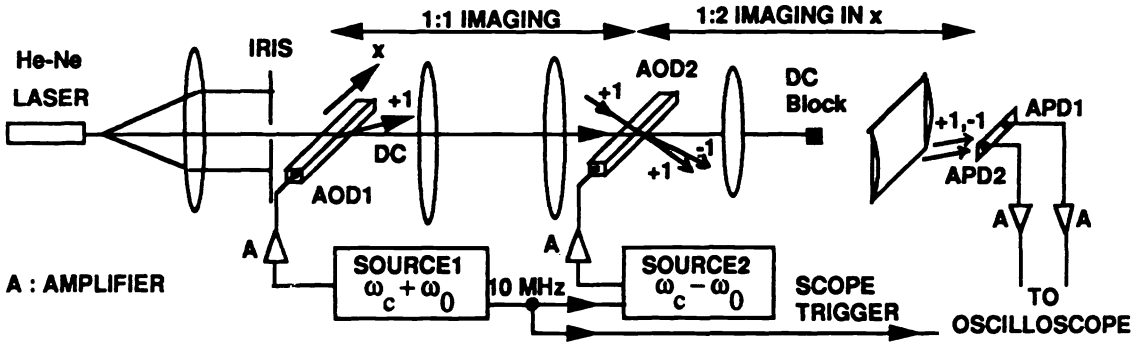

Fig. 1. Basic architecture and experimental setup of the acousto-optic phased array beamformer using single-sideband signals.

dimensions. The 10-cm FL sphere is 15 cm from AOD2, with the detector/image plane along x being 30 cm from the sphere. The DC block is placed 10 cm away or at the front focal plane of the FL=10 cm sphere. The 15-cm cylinder with power in the y, or AOD height, direction is placed 15 cm in front of the 10-cm sphere front focal point, i.e., 25 cm from the sphere. The undiffracted light from the AODs is blocked in the Fourier plane of the 10-cm FL spherical lens, allowing only the +1 and –1 orders to interfere on the detector plane. Considering the 2X magnification along x and 1.5X expansion along y, a light distribution of approximately 32 mm long × 6.8 mm high is formed at the detector plane. On heterodyne detection via the optical detectors, the +1 and –1 orders produce an rf signal on a $2\omega_c$ beat frequency.

Because of the upper and lower sideband nature of the AOD feed signals, the doppler shifts in optical frequency due to the phase control frequency ω_0 cancels out on heterodyne detection. On the other hand, the spatial deflection between the two interfering orders remains dependent on ω_0, and the spatial frequency (in lines per millimeter) of the fringe pattern on the detector plane is given by $2f_0/Mv$, where M is the imaging system magnification, $\omega_0=2\pi f_0$, and v is the acoustic velocity in the AODs. Thus, the rf signal generated by a detector placed along the x direction is $\cos[2\omega_c t+(2\omega_0/Mv)x]$. Note that if an array of equidistant fibers/detectors is placed along the x direction, the rf signal set generated from the detectors satisfies the phase-based beam steering criteria for a linear phased array antenna. Using the SSB AOD drive signals, the antenna carrier $2\omega_c$ and the signal interelement phase shift $\{2\omega_0/Mv\}d$, where d is the inter fiber/detector spacing, become mutually independent. In other words, the antenna carrier can be tuned by varying ω_c, while the phase can be controlled by changing ω_0.

III. Single-Sideband Signal Generation

The required SSB rf signals can be generated in a number of ways. Note that the AOD drive signals must be phase coherent with each other. As shown in Fig. 1, this can be done by externally phase-locking two signal generators to a stable reference source. In our experiment, the 10-MHz external reference from source1 was used as an external reference input signal to source2 to establish the phase coherence. Both signal generators are set at 60 MHz. The phase-shift control frequency ω_0 is introduced by producing a positive frequency offset in source1, with an equal negative frequency offset in source2.

An alternative approach that requires only one microwave source involves using a double sideband (DSB) microwave signal generated by mixing the microwave signal $\cos\{\omega_c t\}$ with the rf phase control signal $\cos\{\omega_0 t\}$. The DSB signal is equivalent to a sum of a USB $(\omega_c+\omega_0)$ signal and an LSB $(\omega_c-\omega_0)$ signal. The desired SSB signal can be fed to its respective AOD after appropriate electronic filtering, which eliminates the unwanted SSB from the DSB signal (see Fig. 2). Optical Fourier plane spatial filtering can also be used to eliminate the undesired sideband [2]. In this case, the DSB signal is fed directly to both AODs, with no electronic filtering. Another possible SSB signal generation technique (Fig. 3) is the phase-shift method [5], which requires a pair of 90-degree phase shifters and two balanced mixers.

IV. Experimental Results

The system in Fig. 1 is set-up on a non-floating optical table. The AODs are driven by 9-V peak @ 50 Ω 60-MHz signals. A pair of Si avalanche photodiodes (APDs), positioned 11.5 mm apart along the x direction at the output image plane, generate 120-MHz carrier signals that are fed to >40-dB gain power amplifiers. The amplifier outputs are

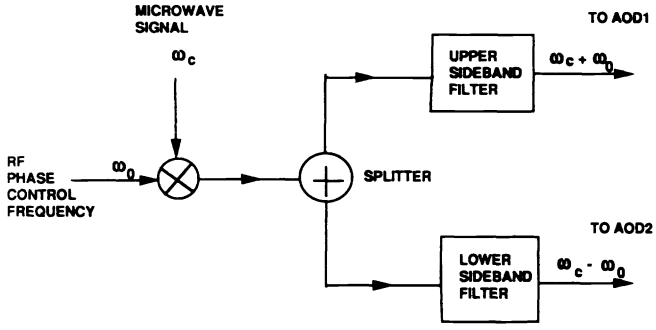

Fig. 2. Single-sideband signal generation using a double -sideband signal and electronic filtering.

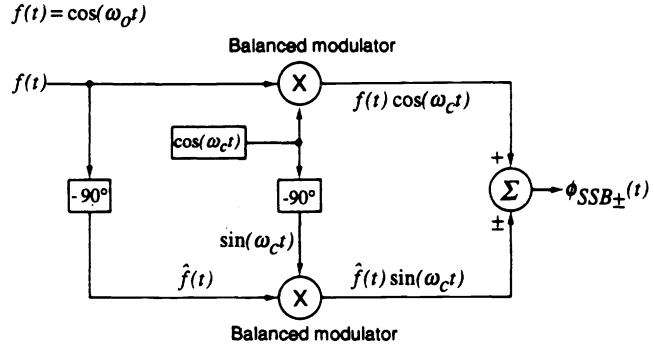

Fig.3. Single-sideband signal generation using the quadrature phase-shift method.

terminated into 50-Ω impedance (analog) oscilloscope channels triggered on the 10-MHz external reference. Fig. 4 shows the excellent phase stability between the 120-MHz carrier signal generated from the interferometric optical processor, and the 10-MHz reference/trigger signal from source1, indicating very good overall signal stability for the system.

Fig. 5 shows the outputs of the APDs as the signals suffer a relative phase shift when ω_0 is varied, with the carrier remaining fixed at 120 MHz. A 180-degree phase shift is achieved for ω_0=170 KHz. The upper trace in the photographs is from an EG&G C30905E APD (APD1), and the lower trace is from a Hamamatsu S2381 APD (APD2), both operating with a bias of 179 V. Fig. 6 shows the desired 0-2π linear phase shift behavior obtained from the system as ω_0 is varied via the SSB approach. The signal dynamic range (DR) obtained from APD2 is 41.2 dB @ 1.3 MHz, with a carrier-to-noise (C/N) >105.1 dB/Hz @ 1.3 MHz. A much better signal quality of 1.82 V p-p @

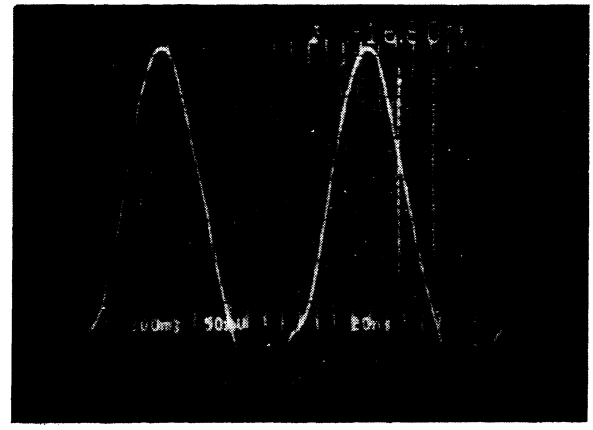

Fig. 4. Analog oscilloscope traces showing the high phase stability between the 120-MHz APD output and the 10-MHz external reference base.

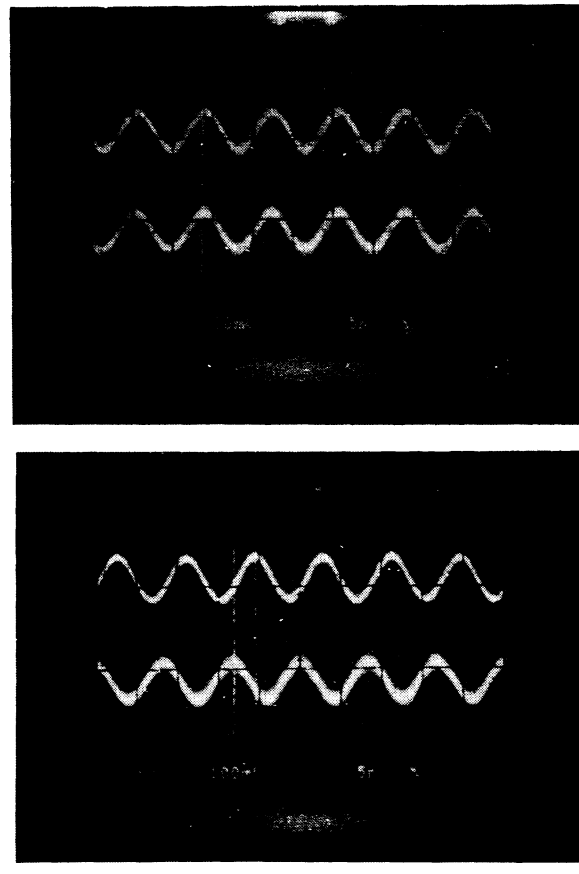

Fig. 5. Oscilloscope traces showing the varying phase shift 120-MHz signals generated by the photodiode pair at the output plane of the processor (plus the 40-dB gain power amplifiers) as the single-sideband control parameter f_o is varied. Upper trace: APD1, 100 mV/div; lower trace: APD2, 5 V/div; time scale: 5 ns/div.

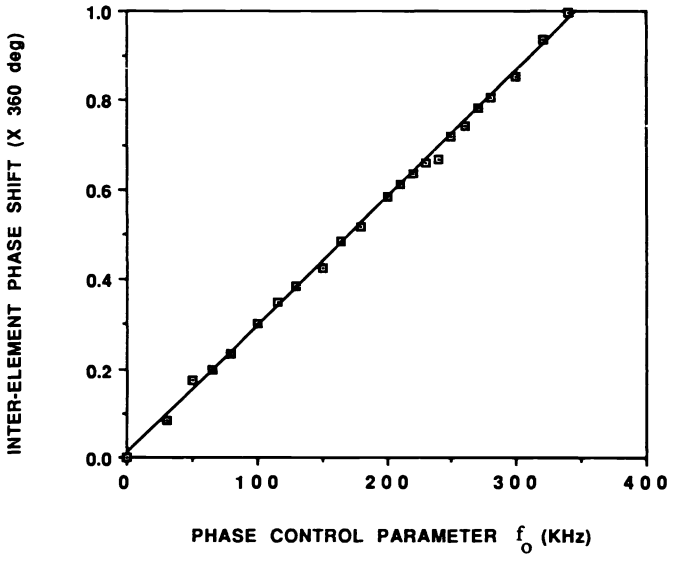

Fig. 6. Experimental plot showing the change in relative phase (0-2p) for the 120-MHz signals from the photodiode pair as the phase control parameter f_o (KHz) is varied.

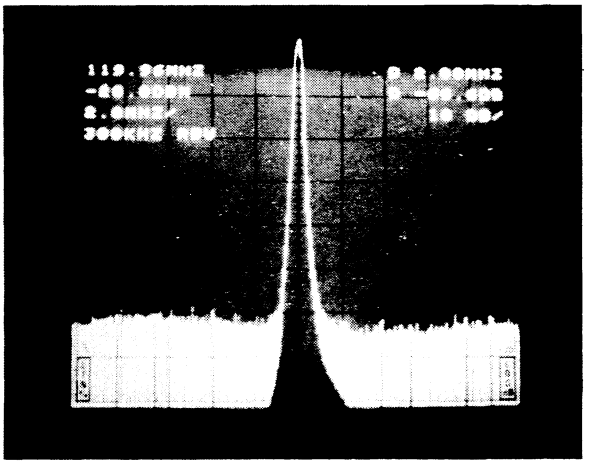

Fig. 7. Spectrum analyzer trace for signal from APD1 positioned near the focus of the FL=10-cm sphere plane, showing a dynamic range DR=66.6 dB @ 2 MHz, using a detector bias of 268 V.

50 Ω (DR=65 dB @ 2 MHz, C/N=126.9 dB/Hz @ 2 MHz) is obtained using the lower noise APD1 still biased at 179 V, and positioned at the front focal plane of the 10-cm sphere in order to utilize higher optical power. This result illustrates that using higher optical power (until the APD noise becomes greater than the detector circuit thermal noise) can indeed generate a signal with better C/N and DR. In addition, the gain of the EG & G APD (near the 10-cm sphere focus) is increased by appropriately biasing the APD at 268 V. This gives a 9.0 V p-p @ 50 W (20.05 dBm) with a DR=66.6 dB @ 2 MHz (Fig. 7). As expected, the carrier is successfully varied by changing ω_c, with the phase shift remaining fixed for a particular ω_o. ω_c can be swept over a very wide bandwidth, as high as 2 GHz, which corresponds to the bandwidth of AODs.

V. Conclusion

We have experimentally demonstrated a processing technique that allows for independent phase and carrier control using SSB signals for the AO phased array antenna beamformer. The experimental results closely agree with the system design, and high performance can be expected with higher power lasers and low noise detectors. An output signal dynamic range of 66.6 dB @ 2 MHz and C/N = 126.9 dB/Hz @ 2 MHz has been measured.

VI. Acknowledgments

Support from GE Aerospace and GE Corporate Research and Development are greatly appreciated.

VII. References

[1] G.A. Koepf, "Optical processor for phased array antenna beam forming," *Proc. SPIE Conf. Opt. Technol. Microwave Appl.*, vol. 477, pp. 75-81, 1984.

[2] N.A. Riza, "Novel acousto-optic systems for spectrum analysis and phased array radar signal processing," chapter 6, Ph.D Thesis, California Institute of Technology, 1989.

[3] N.A. Riza, "Acousto-optic architectures for multi-dimensional phased array antenna processing," *Proc. SPIE Conf. Opt. Technol. Microwave Appl.*, vol. 1476, pp. 144-156, 1991.

[4] N.A. Riza and D. Psaltis, "Acousto-optic signal processors for transmission and reception of phased array antenna signals," *Appl. Opt.*, vol. 30, no. 23, pp. 3294-3303, 1991.

[5] F.G Stremler, *Introduction to Communication Systems*, 2nd ed., Addison-Wesley, p. 243, 1982.